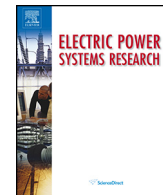




Contents lists available at ScienceDirect

# Electric Power Systems Research

journal homepage: [www.elsevier.com/locate/epsr](http://www.elsevier.com/locate/epsr)



## Power quality analysis in electric traction system with three-phase induction motors

Boško Milešević\*, Ivo Uglešić<sup>1</sup>, Božidar Filipović-Grčić<sup>2</sup>

University of Zagreb, Faculty of Electrical Engineering and Computing, 10000 Zagreb, Croatia

### ARTICLE INFO

#### Article history:

Available online xxx

#### Keywords:

Electric railway  
Power quality  
Induction motors

### ABSTRACT

Three-phase induction motors are widely used in electric traction systems. The impacts of the traction vehicles equipped with three-phase induction motors on power quality are much different from the impacts of vehicles with DC traction motors. In this paper, the effects of the traction vehicle operation with three-phase induction motors on power quality in a 110 kV transmission network are investigated.

The electric traction system 25 kV, 50 Hz and the traction vehicle with three-phase induction motors were modeled including AC/DC rectifier and DC/AC inverter based on IGBT technology. The parameters of those power electronic elements directly determine the current and voltage waveforms, and consequently power quality parameters.

Measurements and calculations of power quality parameters were presented. Three operation modes of traction vehicle were considered including acceleration, constant drive and regenerative braking. During the test drives, the values of total harmonic distortion, unbalance, flicker and power factor were obtained.

© 2016 Elsevier B.V. All rights reserved.

## 1. Introduction

Electric railway systems are essential for the transport of people and goods. Numerous advantages of electric railways have been proven in comparison with other forms of transport, from reliability and safety to the speed and comfort [1]. The development of societies and economics entails the improvement of railways. The most important railway transportation routes are electrified which makes this system more competitive and environmentally more acceptable [2].

An electric railway is a single phase consumer [3]. Operations of traction vehicle may have significant effects on power quality parameters in the power system [4]. One of the most widely used railway electrification systems is 25 kV, 50 Hz. This system is powered from the electric power transmission system and it supplies traction vehicles through contact network. Voltage and current waveforms in the railway system directly depend on the type of traction vehicle, its characteristics and electrical properties [5]. Electric traction vehicles are commonly equipped with DC

motors or three-phase (3f) AC motors [6]. The advantages of 3f induction motors are manifested in possibility for energy recovery during braking or operating on downhill and simplest maintenance. Electric railway system has an influence on systems that ensure reliability of the system (communication subsystem), but also on the systems in the vicinity which are sensitive to disturbances [5,7,8]. Current and voltage waveforms of different traction vehicles cause different disturbances on nearby sensitive systems.

The power transformer at traction vehicle is connected to AC/DC rectifier which is connected to DC link (Figs. 1 and 2). DC voltage is converted by DC/AC inverter to 3f AC voltage and supplies 3f AC induction motor. Power electronics elements, rectifier and inverter consist of thyristors or IGBTs [9]. The power quality parameters and the waveforms of voltage and current are measured on the 110 kV busses. During the measurements only one locomotive was in operation on a feeder supplied from traction substation. That ensures that the other traction vehicles have no impact on the measured values because of their electrical distance.

All measurements were performed during acceleration, constant drive and regenerative braking of electric traction vehicle. Waveforms of electric parameters in different operation modes are compared and deviations from nominal values are found according to the applicable standards [10,11]. The measurements and analysis of power quality parameters in traction substation during the operation of locomotive equipped with 3f induction motors were presented.

\* Corresponding author. Tel.: +385 1 6129 714; fax: +385 1 6129 890.

E-mail addresses: [bosko.milesevic@fer.hr](mailto:bosko.milesevic@fer.hr) (B. Milešević), [ivo.uglesic@fer.hr](mailto:ivo.uglesic@fer.hr) (I. Uglešić), [bozidar.filipovic-grcic@fer.hr](mailto:bozidar.filipovic-grcic@fer.hr) (B. Filipović-Grčić).

<sup>1</sup> Tel.: +385 1 6129 979; fax: +385 1 6129 890.

<sup>2</sup> Tel.: +385 1 6129 714; fax: +385 1 6129 890.

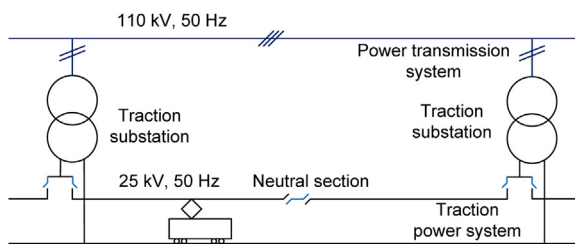


Fig. 1. Electric traction system.

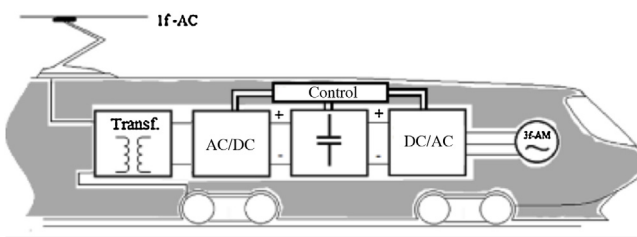


Fig. 2. Electric traction vehicle with an induction motor.

## 2. Operation of traction vehicles with 3f induction motors in electric railway system 25 kV, 50 Hz

The operation of the single-phase 25 kV (50 Hz) electric traction system is significantly different from the electric power system which supplies it [3].

The electric traction system is supplied from electric power system through power transformers located at traction substations. These transformers are connected to two phases of the power transmission system. The traction power supply network is separated by neutral section to the independent sections which are supplied from different traction substations. Fig. 1 shows a principle connection scheme of the 25 kV, 50 Hz electric traction system to 110 kV transmission network.

Electric traction vehicles are powered from contact network via a pantograph and a power transformer that adjusts the 25 kV voltage to a value suitable for induction traction motors (Fig. 2).

In this paper, multi-system traction vehicle supplied by 25 kV, 50 Hz system was analyzed. The nominal drive power of one unit is 6.4 MW and heating power is 900 kVA [12,13]. Fig. 3 shows the measured effective values of current and active/reactive power on 25 kV side. The values of current and power change stepwise and depend on the operation mode. The measured supply current exceeded 300 A, while at the same moment the maximum

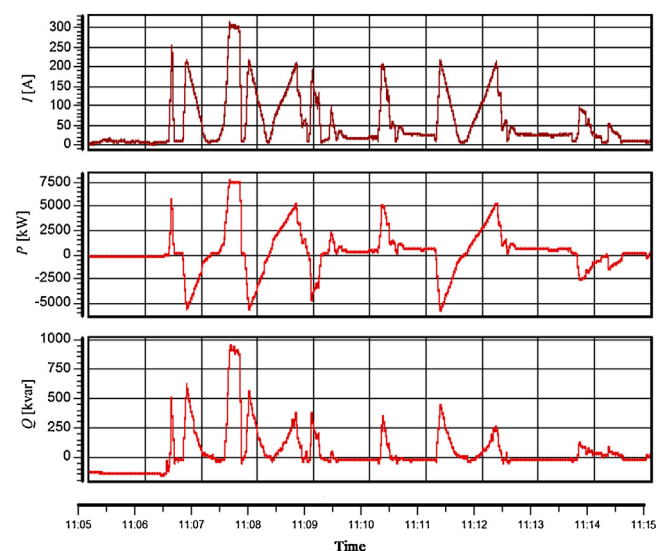


Fig. 3. RMS current, active and reactive power of electric traction vehicle with induction motors.

measured active and reactive powers were 7.5 MW and 950 kvar, respectively. The measured reactive power had a permanent positive sign, whereas active power can have a both positive and negative sign, depending on power flow direction. In the periods when the value of active power is positive, energy flows from the power substation to the traction vehicle while a negative sign indicates the opposite flow of energy. The maximum active power during recuperation braking (energy recovery) was 5.5 MW and has been reached at the moment when the current was 215 A and reactive power was 440 kvar. As expected, the maximum power that can be recovered was less than the maximum power that the vehicle used for the acceleration.

## 3. Model of traction vehicle with induction motors

The model of electric multiple unit of 2 MW continuous power was developed in the ATP software and it includes power transformers at the substation and on the vehicle, IGBT converters, a DC link and an induction motor with rated power 525 kW.

The impedance of 110/25 kV power transformer referred to the 110 kV side is  $R=0.5 \Omega$  and  $L=4 \text{ mH}$  ( $7.5 \text{ MW}$ ,  $u_{k\%}=10\%$ ). Contact network impedance is  $0.181+j0.447 \Omega/\text{km}$ . The DC link was modeled by a capacitance ( $C=36 \text{ mF}$ ) and an inductance

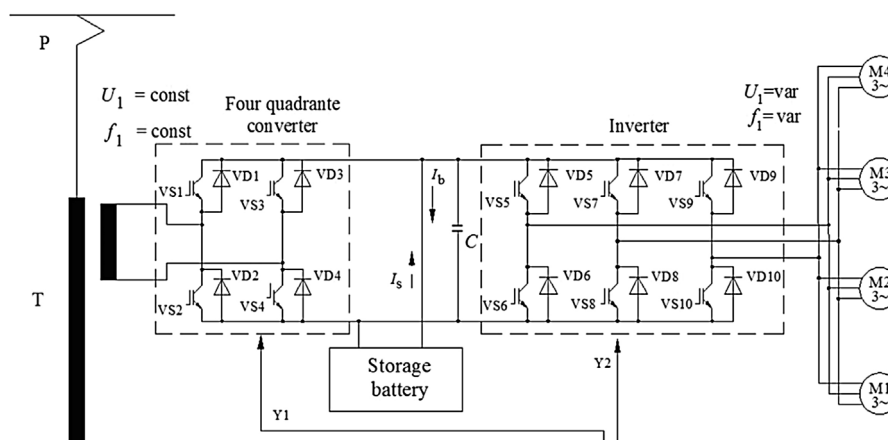
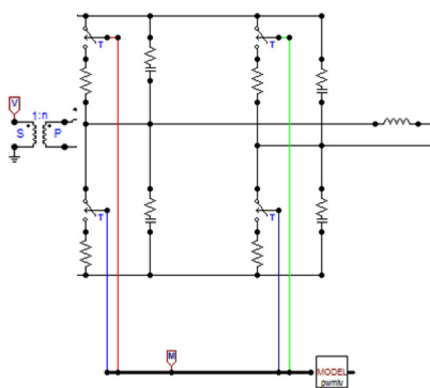
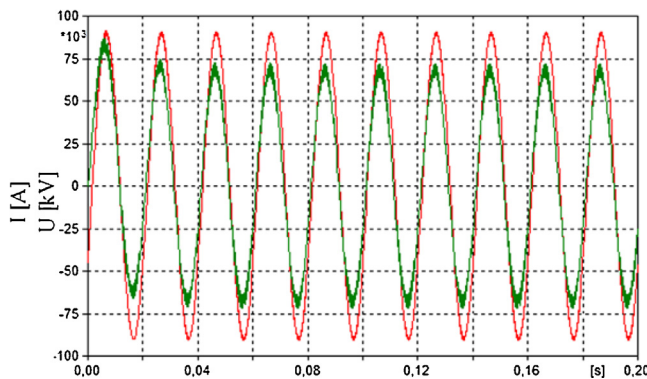


Fig. 4. Electrical scheme of traction vehicle with induction motors [14].



**Fig. 5.** Model for calculation in ATP.



**Fig. 6.** Current (green) and voltage (red) on contact network on the 110 kV side. (For interpretation of the references to color in this figure legend, the reader is referred to the web version of this article.)

( $L=0.007 \text{ mH}$ ). Electrical scheme and model for calculation are shown in Figs. 4 and 5.

Rectifier consists of four switches controlled by PWM (Pulse-Width Modulation) signal. The algorithm which generates the control PWM signals contains the modulation signals and the carrier signal (triangular wave). The triangular signal was modeled and its frequency is an odd multiple of the modulation signal. The frequency of the input signal is determined by the frequency of the contact network.

Inverter contains three branches each with two switches. The control of switches operation is realized by a PWM module. The developed model of traction vehicle enables the analysis of any motor operation frequency. The current and voltage waveforms on 110 kV side of traction substation at the frequency 50 Hz are shown

in Fig. 6. Current waveform shown in the same figure is multiplied by 10.

These waveforms show that the fundamental power frequency of 50 Hz is supplemented by some higher harmonics. FFT (Fast Fourier Transformation) is calculated from the obtained voltage and current waveforms (Figs. 7–9) in order to analyze the power quality parameters.

The results depicted in Figs. 7–9 show that from all higher harmonics the 41st harmonic had a maximum magnitude of 30 V on 110 kV side which is about 0.03% of the magnitude of fundamental harmonic. The same harmonic on 25 kV side reached 16 V or 0.04% of fundamental harmonic. Also, the maximum higher harmonic of the current was 41st, with a magnitude of 2.7% of fundamental harmonic.

#### 4. Measurement and analysis of voltage and current waveforms

The measurements of power quality parameters were performed on 110 kV side in the electric traction substation. The switching arrangement of substation and the locomotive position during the measurements are shown in Fig. 10.

Two 110 kV overhead lines are connected to the traction substation. The transmission and traction systems are connected via power transformers 110/25 kV with nominal power 7.5 MVA. During the measurements only transformer A was in operation. The one locomotive traveled from point M1 to point M2 on the section B.

Supply and regenerative currents and voltages between phases L2 and L3 on 110 kV side were measured in the transformer bay. Also, the values of power factor, unbalance and total harmonic distortion (THD) were observed.

In this chapter the waveforms of voltages and currents are presented. The waveforms depend on the operation mode (acceleration, constant drive or regenerative braking). Results are presented for all three operation modes. Also, the comparison tables with the content of each harmonic are given.

The measurements are performed before, during and after locomotive operation. By comparing the results obtained in all three periods is clear that the current and voltage distortions are mainly caused by operation of the observed traction vehicle.

##### 4.1. Voltage and current during the acceleration

The voltage and current waveforms during acceleration are presented in Fig. 11. Phase shift between voltage and current is very low. Figs. 12 and 13 show harmonic spectrum of those waveforms obtained by FFT.

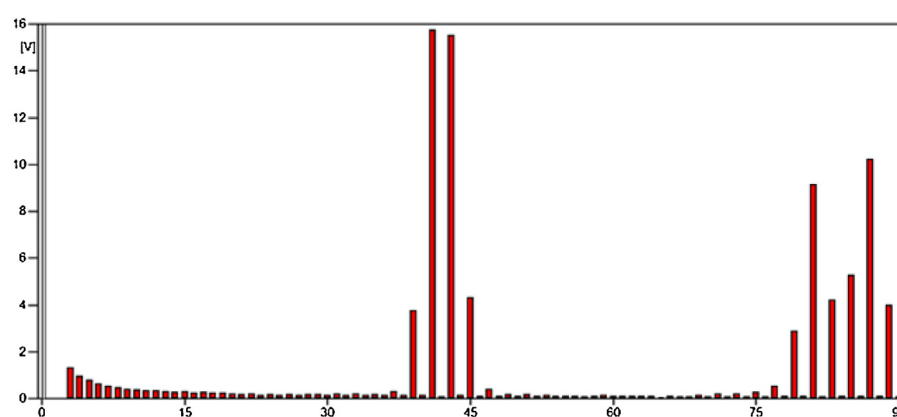


**Fig. 7.** Voltage FFT on the 25 kV side (harmonics 3rd to 90th of power frequency).

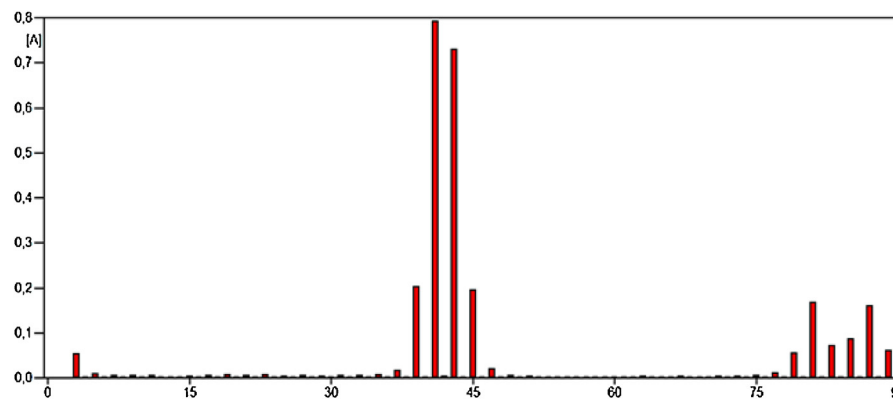


**Fig. 8.** Current FFT on 25 kV side (harmonics 3rd to 90th of power frequency).

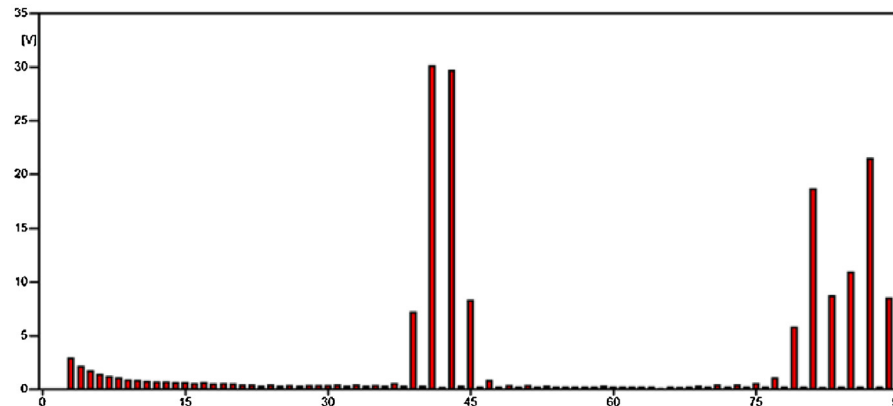


**Fig. 9.** Voltage FFT on 110 kV side (harmonics 3rd to 90th of power frequency).

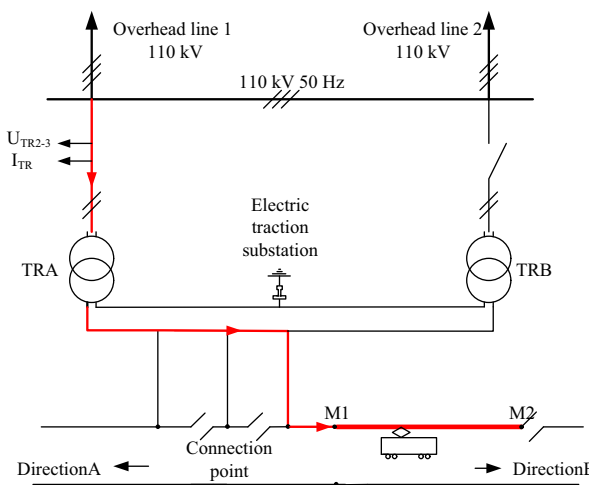


**Fig. 10.** Electric traction substation connection and train position.

#### 4.2. Voltage and current during the constant drive

Voltage and current waveforms in constant drive operation mode are depicted in Fig. 14. Similarly as in the case of acceleration mode, phase shift is very low. FFT of obtained waveforms is presented in Figs. 15 and 16.

#### 4.3. Voltage and current during the regenerative breaking

In operation mode of regenerative breaking (energy recovery) phase the shift between voltage and current was 180°. In Fig. 17,

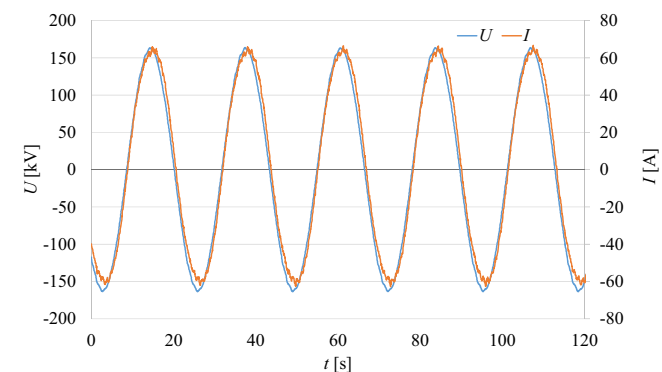


**Fig. 11.** Voltage and current through the power transformer during the acceleration.

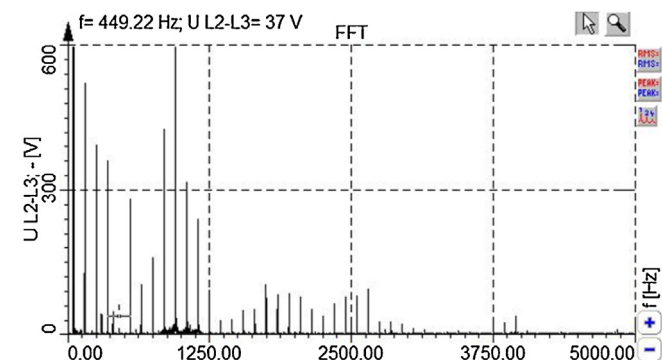


**Fig. 12.** FFT of voltage during the acceleration.

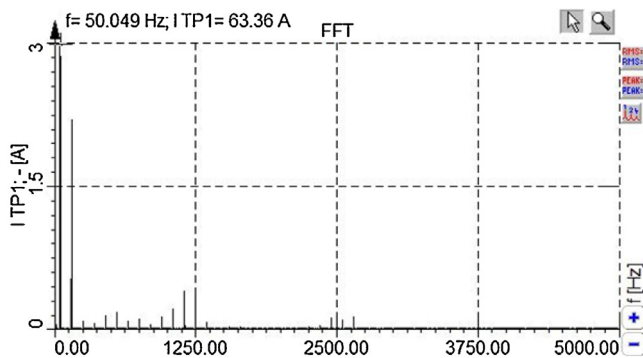


Fig. 13. FFT of current during the acceleration.

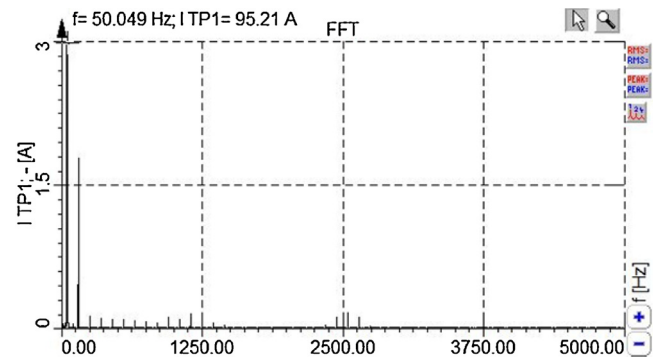


Fig. 16. FFT of current during the constant drive.

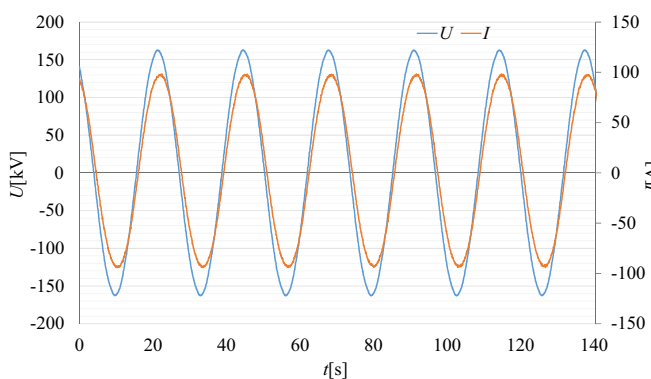


Fig. 14. Voltage and current during the constant drive.

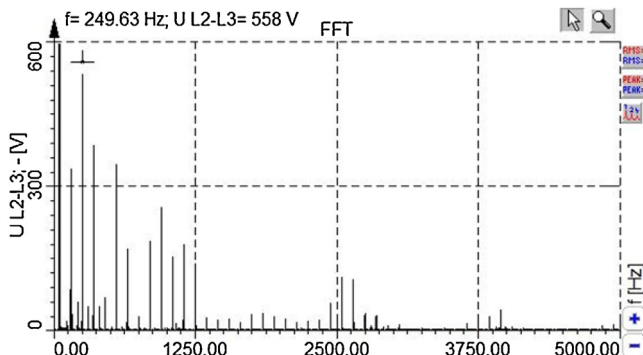


Fig. 15. FFT of voltage during the constant drive.

waveforms of voltage and current flowing through power transformer are shown. Voltage had almost ideal sinusoidal waveform, but the current contained higher harmonics of significant magnitude. FFT up to 100th harmonic of power frequency is shown in Figs. 18 and 19.

In Table 1, the magnitudes of each voltage harmonic depending on all three operation modes are given, with regard to previous figures.

The measured voltage had a significant content of higher harmonics in all operation modes. Fig. 20 shows voltage THD in all phases on 110 kV side. THD of line voltage connected to power transformer reached 1.35%. The maximum values of THD were observed in acceleration and breaking periods. In phase L1, which is not connected to railway system, THD had almost a constant value of 0.7%. This fact shows that electric railway vehicles equipped with 3f induction motors have an important effect on voltage waveform. However, the results presented in this paper were much lower than the values allowable in standards.

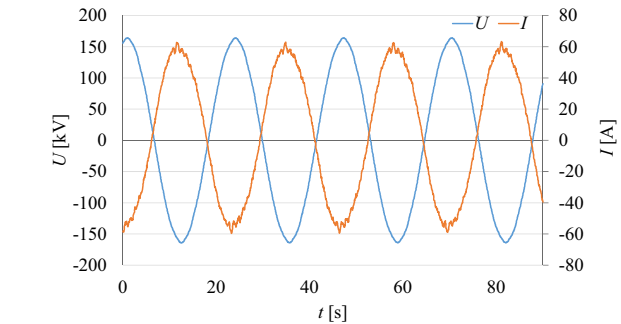


Fig. 17. Voltage and current during the regenerative breaking.

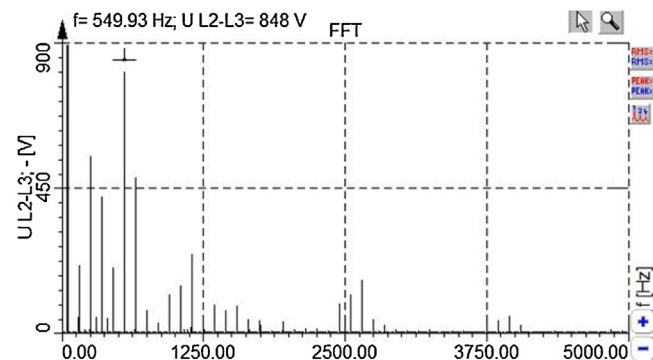


Fig. 18. FFT of voltage during the regenerative breaking.

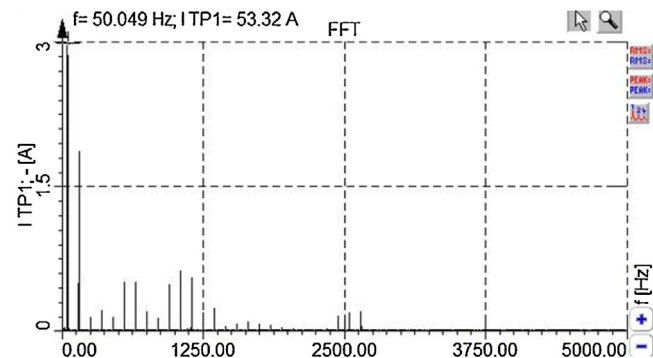


Fig. 19. FFT of current during the regenerative breaking.

In Table 2, the magnitudes of each current harmonic in all three operation modes are given, with regard to previous figures.

The measured current had a significant content of higher harmonics in all operation modes. The value of current THD in all three phases on 110 kV side is presented in Fig. 21. THD of current

**Table 1**

Magnitude of voltage harmonics depending on operation mode.

Harmonic order $\nu$	Operation mode magnitude [%]		
	Acceleration	Constant drive	Recuperation
1	100.00	100.00	100.00
3	0.31	0.20	0.13
5	0.26	0.37	0.34
7	0.25	0.22	0.28
9	0.12	0.02	0.13
11	0.28	0.19	0.53
13	0.03	0.13	0.30
15	0.12	0.01	0.05
17	0.29	0.05	0.02
19	0.26	0.03	0.08
21	0.10	0.02	0.09
23	0.11	0.10	0.16
25	0.05	0.05	0.04
27	0.03	<0.02	0.06
29	0.02	<0.02	0.04
35	0.03	<0.02	0.05
39	0.48	<0.02	<0.02
41	0.05	<0.02	<0.02
43	0.03	<0.02	<0.02
45	0.03	<0.02	<0.02
47	0.05	<0.02	<0.02
49	0.05	0.04	0.06
51	0.05	0.07	0.08
53	0.07	0.06	0.10

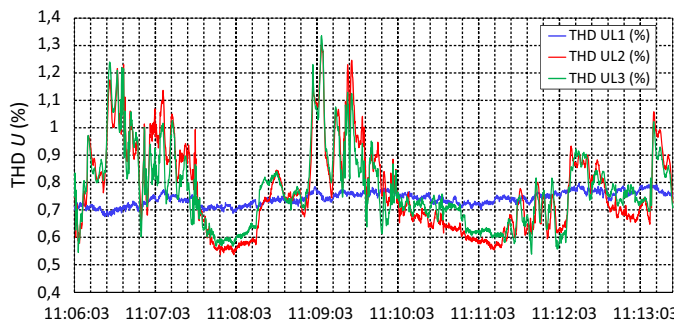


Fig. 20. Voltage total harmonic distortion on the 110 kV side.

flowing through power transformer reached 2.7%. Maximal values of THD were observed during the acceleration and breaking periods. As it is shown in Figs. 20 and 21, voltage and current THDs are mainly due to operation of traction vehicle, since the electric railway system is connected between the phases L2 and L3.

Information about instrument transformers errors, which can be obtained from frequency response and harmonic distortion tests, were not available to authors'. The magnitudes of voltage and current harmonics at higher frequencies shown in Tables 1 and 2 are

**Table 2**

Magnitude of current harmonics depending on operation mode.

Harmonic order $\nu$	Operation mode magnitude [%]		
	Acceleration	Constant drive	Recuperation
1	100.00	100.00	100.00
3	3.71	1.88	3.54
5	0.15	0.14	0.28
7	0.10	0.12	0.43
9	0.26	0.13	0.30
11	0.22	0.11	0.98
13	0.22	0.09	1.00
15	0.17	0.09	0.41
17	0.20	0.04	0.24
19	0.36	0.06	0.92
21	0.15	0.09	1.20
23	<0.10	0.39	1.09
25	0.61	0.19	0.34
27	0.24	0.07	0.45
29	0.10	<0.10	<0.10
35	<0.10	<0.10	<0.10
39	<0.10	<0.10	<0.10
41	<0.10	<0.10	<0.10
43	<0.10	<0.10	<0.10
45	<0.10	<0.10	<0.10
47	<0.10	<0.10	<0.10
49	0.22	0.03	0.30
51	0.22	0.19	0.38
53	0.26	0.12	0.40

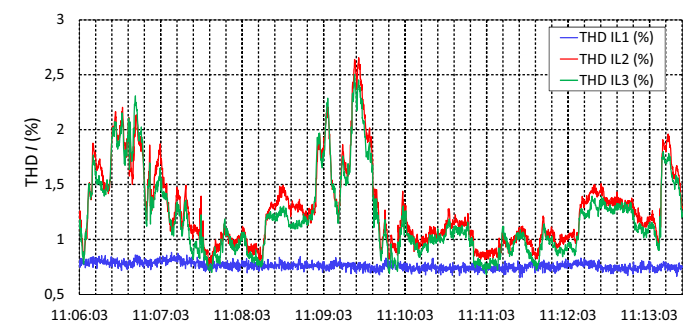


Fig. 21. Current total harmonic distortion on the 110 kV side.

presented only to show the relative ratio between harmonics. It can be concluded that the constant drive operation causes less harmonics compared to acceleration and recuperation operations.

#### 4.4. Measurement of unbalance and flicker

Unbalance and flicker were measured on 110 kV level. The measurements were performed during two drives, each lasting 7 min.

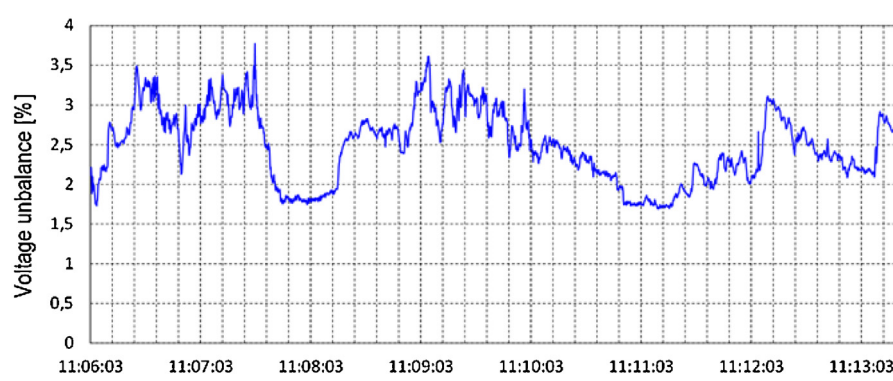


Fig. 22. Voltage unbalance on the 110 kV side.

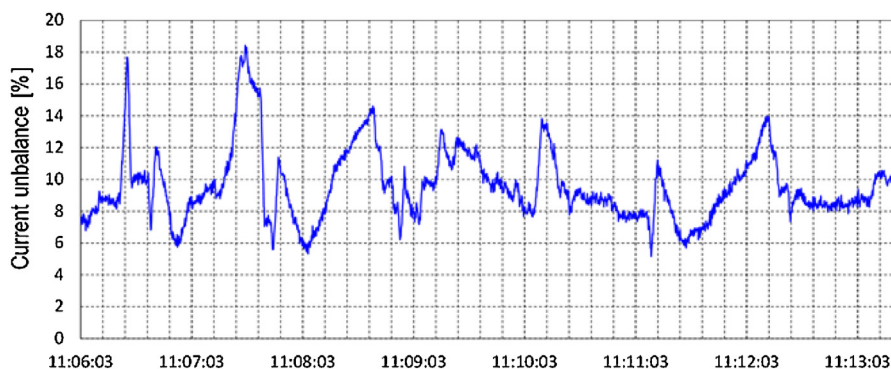


Fig. 23. Current unbalance on the 110 kV side.

**Table 3**

Short time flicker values on 110 kV side.

Phase	$P_{st}$
L1	0.1090
L2	0.1046
L3	0.1042

The drives were regulated according to the measuring requirements with frequent acceleration and breaking periods.

For the period depicted in Fig. 3, the values of voltage (Fig. 22) and current unbalance (Fig. 23) were obtained at connection point of overhead line 2. The unbalance is determined as the percentage ratio of negative sequence voltage to positive sequence voltage and it is comparable with [15,16]. The values of short time flicker are also presented in Table 3.

The voltage and current unbalance at the connection point of the electric railway to the transmission network were lower than 3.8% and 19%, respectively. In order to determine the influence of the traction vehicle on unbalance in the 110 kV network, measurements should be performed during one week according to [17]. 95% of the 10 min mean r.m.s. values of the negative phase sequences should be under 2%.

Short time flicker values per phases are given in Table 3. Considering the maximum permitted values defined in standards, the measured values of short time flicker were below limits [18].

## 5. Conclusions

In this paper, the monitoring of power quality parameters at the point of electric railway system connection to the transmission system was described. The operation of the electric traction system 25 kV, 50 Hz supplied from the traction substation 110/25 kV was presented. The impact of the 3f traction motors on the transmission network was investigated by the measurements of power quality parameters (THD, unbalance, flicker).

A railway system with a traction vehicle equipped with 3f induction motor was developed in EMTP-ATP. The waveforms of voltage and supply current were analyzed. In the calculations the 41st and 42nd harmonics of power frequency were identified with the highest magnitude while in the measurements 3rd, 21st, and 53rd harmonic were significant. That mostly depends on the converters characteristics.

Voltage and current waveforms were analyzed during three operation modes of the electric traction vehicle: acceleration, constant drive and regenerative breaking. It is clear that the 3f traction induction motors have an impact on the power quality parameters especially during acceleration and breaking. However,

operation in energy recovery mode results with the most significant impact.

The values of THD, unbalance and flicker obtained by measurements were below the limits prescribed in standards. From the standpoint of power quality and energy consumption efficiency, 3f induction motors in electric traction system have many advantages and their use is increasing.

## Acknowledgments

This work has been supported in part by the Croatian Science Foundation under the project “Development of advanced high voltage systems by application of new information and communication technologies” (DAHVAT).

The authors gratefully acknowledge the contributions of the Croatian Transmission System Operator Ltd. and HŽ Infrastruktura Ltd. for enabling the measurements.

## References

- [1] S. Frey, Railway Electrification Systems & Engineering, White World Publications, Delhi, 2012.
- [2] I. Uglešić, M. Mandić, Napajanje Električne Vuče, Graphis, Zagreb, 2014.
- [3] Y. Osura, Y. Mochinaga, H. Nagasawa, Railway electric power feeding systems, Jpn. Railway Transp. Rev. 16 (June) (1998) 48–58.
- [4] R.C. Dugan, M.F. McGranahan, S. Santoso, H. Wayne Beaty, Electric Power Systems Quality, third ed., McGraw-Hill, New York, USA, 2012.
- [5] B. Milesević, Electromagnetic Influence of Electric Railway System on Metallic Structures, University of Zagreb, 2014 (Ph.D. Dissertation).
- [6] T. Achour, M. Pietrzak-David, M. Grandpierre, Service community of an induction machine railway traction system, in: XIX Int. Conference on Electric Machines—ICEM, Rome, 2010.
- [7] International Telecommunication Union, Directives Concerning the Protection of Telecommunication Lines Against Harmful Effects from Electric Power and Electrified Railway Lines, vol. IV, International Telecommunication Union, Geneva, 1989.
- [8] A. Zupan, A. Tomasovic Teklic, B. Filipovic-Grcic, Modeling of 25 kV Electric Railway System for Power Quality Studies, EuroCon, Zagreb, 2013 (2013).
- [9] W. Buchberger, Die neue schnellfahrende Mahrsystem—Hochleistungslok 1216 der OBB, September 2004, (<http://www.br146.de/SiemensPdf/Rh1216-oebb.pdf>) (January 2014).
- [10] IEEE Standard Association, IEEE Recommendation Practice and Requirements for Harmonic Control in Electric Power Systems, IEEE Std 519™-2014, New York, NY, 2014.
- [11] N. Cho, Allocation of Individual Harmonic Emission Limits in Accordance with the Principles of IEC/TR 61000-3-6, Georgia Institute of Technology, 2013 (Ph.D. Dissertation).
- [12] Schweinfurt, Germany author: Krauss-Maffei Krauss-Maffei, FAG Wheelset Bearings in the High-Power Locomotive “TAURUS”, Examples of Application Engineering Publ. No. WL 07 510 EA, ([http://www.schaeffler.com/remotemedien/media/\\_shared.media/08.media.library/01\\_publications/\\_schaeffler\\_2/publication/downloads\\_18/wl\\_07510\\_de\\_en.pdf](http://www.schaeffler.com/remotemedien/media/_shared.media/08.media.library/01_publications/_schaeffler_2/publication/downloads_18/wl_07510_de_en.pdf)), Schweinfurt, Germany, January 2015.
- [13] Siemens AG Transportation Systems, Führerstand der 1116 Taurus, January 2014, (<http://www.z21.eu/content/download/625/4858/file/Z21%20F%C3%BChrerstand%20der%201116%20Taurus.pdf>).

- [14] L. Liudvinavicius, L.P. Lingaitis, Management of locomotive tractive energy resources, in: Energy Management Systems, InTech, Rijeka, Croatia, August, 2011.
- [15] M. Krisna, Types of power quality disturbances on AC electric traction drives: a survey, *J. Cent. Power Res. Inst.* 9 (June (2)) (2013) 191–196.
- [16] S.V. Sangle, C.H. Malla Reddy, A novel technology for harmonics and unbalance compensation in electric traction system using direct power control method, *IJIERT: Int. J. Innov. Eng. Res. Technol.* 2 (8) (2015) 1–10.
- [17] European standard EN 50160, Voltage Characteristics of Electricity Supplied by Public Electricity Networks, European Committee for Electrotechnical Standardization (CENELEC), Brussels, Belgium, 2010.
- [18] M.H. Albadi, A.S. Hinai, A.H. Al-Badi, M.S. Al Riyami, S.M. Hinai, R.S. Al Abri, Measurements and evaluation of flicker in high voltage networks, in: Int. Conference on Renewable Energies and Power Quality, April 2014, Cordoba, Spain, 2014.